Chapter 3

Operando Structural Characterization of the E-ALD Process Ultra-Thin Films Growth

Andrea Giaccherini, Roberto Felici and Massimo Innocenti

Additional information is available at the end of the chapter

http://dx.doi.org/10.5772/67355

Abstract

Spanning from nanoelectronics to new solar energy materials, technological development in the recent years requested highly controlled nanostructured surfaces, ultra-thin films, and 2D structured materials. In general, although very favorable from a full life cycle assessment (FLCA) standpoint, electrodeposition hardly allows to obtain the high order required by recent technologies. In particular cases, the electrodeposition enables the deposition of atomic layers by means of surface limited reactions (SLRs). By exploiting SLRs, it is possible to define layer-by-layer deposition scheme of different atomic layers; we refer to these schemes as electrochemical atomic layer deposition (E-ALD) and when the growth of the film is epitaxial with the substrate, the techniques are called electrochemical atomic layer epitaxy (ECALE). Aiming at characterizing structure and growth of materials grown by means of E-ALD, surface analysis techniques apply better. In particular, surface X-ray diffraction (SXRD) with high brilliance synchrotron sources enables the operando structural analysis in electrochemical environment. In recent years, several works on the operando surface characterization by means of SXRD have been reported. Thanks to novelties in the field of operando SXRD experiments, semiconducting systems were studied, such as single and multilayer of CdS and Cu_2S.

Keywords: ECALE, E-ALD, thin films, 2D materials, SXRD

1. Introduction

A fundamental aim of material research and surface science is the development of deposition techniques of compound semiconductors with low impact from either the energetic or environmental points of view. These techniques should ensure a high structural control for the

engineering of nanostructures such as quantum dots, quantum well, superlattices, and thin films still preserving the crystalline properties of the grown material. The bottom-up approach is renowned as very favorable for the synthesis of such materials in the form of dispersed nanoparticles from molecular precursor, usually involving several steps and the addition of surfactants to the reaction environment. Since most of these products, obtained following these pathways, are in form of powders, the production of solid-state devices requires several steps for the deposition of the materials. In this context, electrodeposition has the advantage of the direct production of the films from the molecular precursors. In any case, electrodeposition hardly results in highly ordered materials as requested by recent technologies based on semiconductor. However, in specific conditions, electrodeposition enables the assemblage of atomic layers by means of surface limited reactions (SLRs). SLRs give the opportunity of exploiting layer-by-layer deposition of different atomic layers, leading to one of the most clean and energy saving approaches, electrochemical atomic layer epitaxy (ECALE) [1], for the growth of heterostructures. ECALE could be also referred in general as electrochemical atomic layer deposition (E-ALD) since in some cases the growth, though based on under potential deposition (UPD) processes or on any SLR, cannot be rigorously considered epitaxial. Hence, E-ALD joins highly ordered products with the direct access to the final material in the context of the bottom-up approach in a very clean reaction environment. E-ALD has been proven to be very effective for the electrodeposition of ultra-thin films of semiconducting materials. In recent years, thin films of binary [2–5] and ternary semiconductors [6–9] were successfully obtained. E-ALD requires very low energy consumption, diluted solutions, room temperature, and atmospheric pressures. Thus, it can be employed for the sustainable large-scale production of these materials. This is particularly interesting for photovoltaics application, where the improvements of the full life cycle assessment (FLCA) are considered a crucial aspect for the possible large-scale production of new materials [10]. In this context, it is very crucial to study and understand the growth mechanism together with the detailed analysis of the structural features of the resulting thin films. For this purpose, surface analysis techniques play an important role. Among them, surface X-ray diffraction (SXRD), with high brilliance synchrotron sources, enables the operando structural analysis in electrochemical environment during the E-ALD growth and discloses the structural features of such systems during the deposition process. In recent years, several works on the operando characterization of ultra-thin films have been reported thanks to the development of specifically designed flow cells and automated apparatus to perform 100 or more growth cycles in few hours.

2. E-ALD for semiconducting materials

Materials overcoming the properties of silicon-based semiconducting materials are very widely researched. In particular, the interest is devoted toward materials with optoelectronic and electronic properties, in a broad range, able also to work in severe conditions. In this context, compound semiconductors are promising candidates. They result from the combination of two or more elements. The ones formed by elements of the groups symmetrical to the IV group, namely the III–V compound semiconductors are among the most studied. Epitaxy is

http://dx.doi.org/10.5772/67355

generally expected to enhance their semiconducting proprieties, such as mean free path and charge carrier mobility. Moreover, epitaxial growth is necessary to obtain superlattices, i.e., materials with a periodic modulation of structure or composition and crystallographic coherence with respect to the atomic planes [11]. For example, without the crystallographic coherence, a bilayer ZnSe/CdSe film or a sequence of multiple layers of ZnSe, CdSe is not called a superlattice, but simply a heterojunction or a multilayer system. In this field, superlattices are of increasing interest, since it is possible to tailor their properties even at the nanoscale, where they are exhibiting quantization effects. The growth of perfectly flat, ultrathin, and even 2D sheets of material is a stringent requirement for the functionality of multilayers or superlattices. E-ALD provides a sustainable solution got the growth of high-quality 2D materials with well-controlled periodicities.

E-ALD constitutes an easy way to deposit suitable ultrathin films and 2D materials alternating atomic layer of different elements in a very straightforward manner. For these reasons, since its infancy, the E-ALD study has been carried on compound semiconductors, with a specific focus on compound semiconductors based on elements of the II–VI groups. **Figure 1** depicts a general scheme for the E-ALD of a ternary chalcogenide, this can be obtained by alternating SLR steps of metals (M1, M2) and chalcogenides (C).

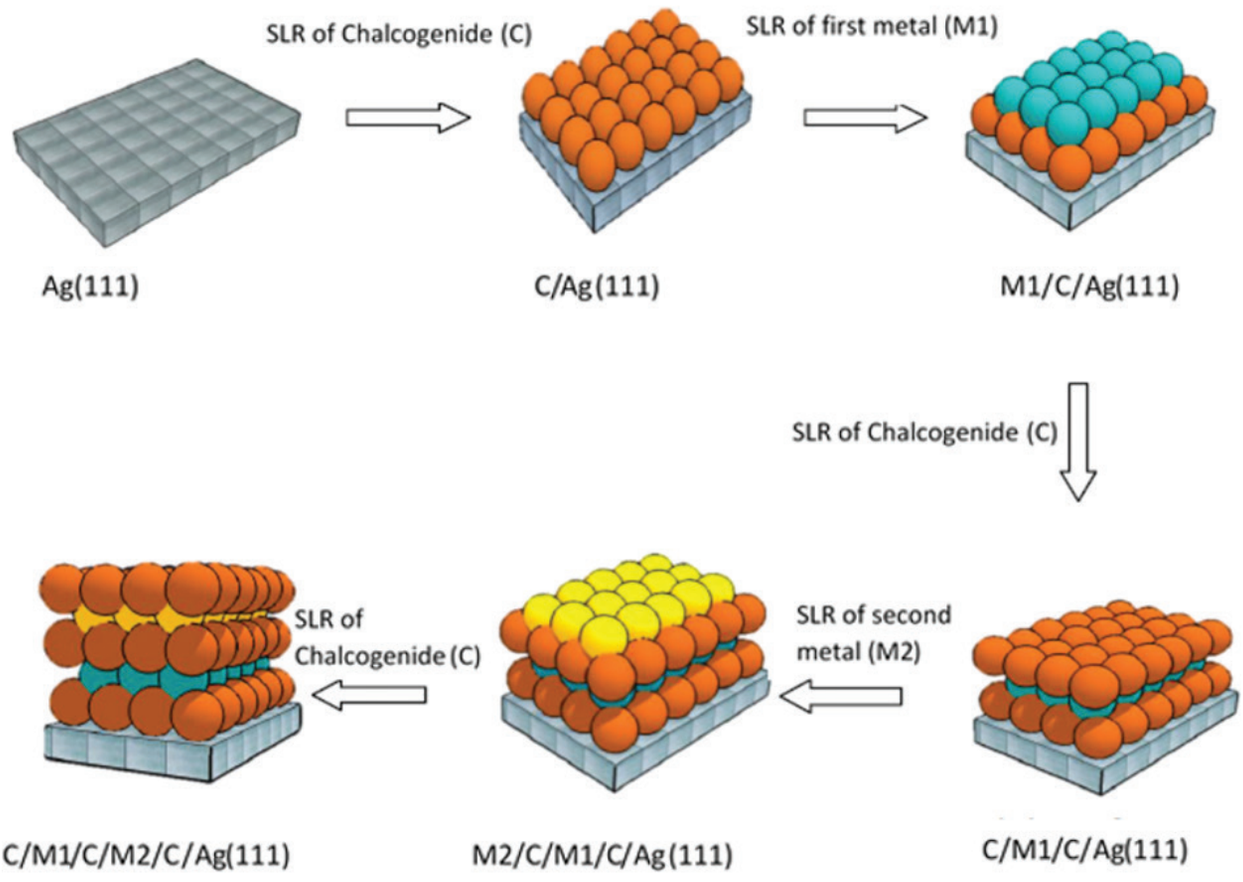

Figure 1. General scheme for an E-ALD process aimed to grow a ternary chalcogenide. C, M1 and M2, respectively, stand for an atomic layer of chalcogenide, first metal in the scheme and second metal in the scheme.

In order to tailor the stoichiometry of the compounds, it is possible to define schemes with different number of steps for the two metals, as will be discussed in Section 2.2.2 for Cu_xZn_yS. The E-ALD procedure requires a thorough knowledge of the separated SLRs (often UPD—under potential deposition) involved in the deposition of the metals over the nonmetals and vice versa. An open issue is the exact definition of the driving force leading these processes. It is very widely accepted that the main contribution to the driving force is the negative free energies change involved in the interaction with the electrodic surface and in the formation of a thermodynamically stable compound. However, the surface can change during the growth due to formation of the crystal, and it is possible to think of a change also in the driving force when a relatively thick crystal is grown. As reported by almost every paper on this topic, it is worth to notice that, usually, the first step of the E-ALD process is the deposition of an atomic layer of chalcogen (or of the nonmetal in general) over the bare metal substrate. Reasonably, the experimental conditions for the deposition change while increasing the thickness of the deposit. For instance, in the growth of crystals, the accumulation of the elastic energy into the lattice is a nonfavorable contribution to the driving force. This is a well-known issue leading to different growth mechanisms and related morphology. Usually, in the case of the E-ALD process, these effects do not prevent the compound formation. Generally speaking, the changes are in the sense of decreasing the amount of deposition and then the total time of the process increases. This can prevent the deposition of some materials, as CdTe and InAs, with a thickness of practical relevance. In other cases (such as the deposition of Cu_2S), the deposition of the copper layer, implying the reduction of copper ions from the solution, may result in more complex reactions implying the formation of some intermediate compounds and the deposition cannot be accounted strictly by the UPD process. Several experimental evidences for these controversial aspects have been reported and they will be discussed in the following pages. It is worth to notice that they reveal a complex mechanism for the formation of chalcogenides by means of E-ALD. The complexity of these processes occurring during the growth is the reason why we prefer to refer to the E-ALD steps with the acronym SLR rather than using UPD.

In this work, we focus on the deposition of chalcogenides on a Ag single crystal, usually on the Ag(111) surface if not specifically indicated. All the potentials repoeted here are referred to the Ag/AgCl(KCl sat.) reference electrode.

2.1. Cadmium-based compound semiconductors

Cadmium chalcogenides have been among the first compound semiconductors to be deposited by means of E-ALD due to their interesting electronic properties and favorable electrochemical characteristics.

2.1.1. CdS

One of the first chalcogenides electrodeposited by E-ALD is the CdS, extensively studied on several different single crystals. The E-ALD process for CdS on Ag(111) has been verified to be epitaxial and does not require the formation of any intermediate compounds [12, 13]. Its deposition can be considered a genuine ECALE process. It starts with the oxidative UPD of the sulfur ions on the metal surface. It is worth mentioning that the structure of the resulting

http://dx.doi.org/10.5772/67355

sulfur layer has been deeply studied by means of scanning tunneling microscopy (STM) measurements. The second step of the ECALE process is the UPD deposition of cadmium on top of the Ag(111)/S. The charge associated with each layer of either Cd or S corresponds to 0.165 monolayers (referred to as the ideal covering of a layer of the Ag(111) substrate). STM measurements confirm that the fractional coverage of the Cd and S cycles on top of the Ag(111)/S from the 3/7 of the first S layer to the 1/7 (consistent with the coulomb-metric measurement). The epitaxial growth is actually confirmed by the STM images of the first four atomic layers, whereas the unit value of the S/Cd ratio for the successive layers strongly suggests that the epitaxial growth is maintained in these further layers. Moreover, the charge deposited was verified to be linear with the number of ECALE cycles [2] for ECALE scheme as long as 50 cycles. Thus, the results are consistent with the layer-by-layer mechanism proposed for the ECALE process. CdS shows a discrepancy between the deposition on Au(111) and Ag(111). Shannon and Demir reported a (333) structure with a Cd–Cd distance of 4.3 Å for the Cd layer on top of the S layer deposited on Au(111) [14]. This structure is much more compact than the one obtained by our group (0.76 nm for both Cd–Cd and S–S distances) and that difference cannot be ascribed to a difference in lattice constants of Ag and Au since they are practically identical. We proposed that the difference could be ascribed to the different structure of the S layer in contact with the metallic substrate. In fact, the S layer on Au(111) forms a structure with a coverage of one-third, while in the experimental condition we defined on Ag(111) forms a site occupied by a triplet of sulfur atom (coverage of 3/7) and is therefore much more compressed. Thus, Ag denotes a higher affinity with S, resulting in a CdS structure, as determined by STM, corresponding to the basal planes of both wurtzite and zinc blende; these two structures are very similar on the basal plane, and it is not possible to distinguish them by means of STM studies of the first E-ALD cycles. SXRD experiment clarified the structure of CdS and showed that high crystalline quality of the CdS films grown on different surfaces [12, 13]. On the Ag(111), the growth films present only the hexagonal wurtzite structure, while on the other low index planes, a mixture of the hexagonal wurtzite and cubic zinc-blende phases is present.

2.1.2. Other Cd-based chalcogenides

It has been shown that a one-step oxidative SLR is not possible for selenides and tellurides. The E-ALD process for CdSe involves the same steps of the CdS, but the experimental conditions are very different [15]. Hence, the deposition of the Se layer is usually obtained by means of a two-step process [15]. The first implying a massive deposition of a Se film on the Ag(111) followed by reduction of all but the adlayer of Se on the Ag(111) surface. A 1:1.3 (Cd:Se) growth on Ag(111) has been achieved, a tentative explanation is that the transition to a less compact Se structure can occur during the stripping of the bulk Se. The peak related to the transition is probably overlapping with the bulk Se reduction peak. Hence, a lower than expected covering of the substrate is achieved, and consequently, a Cd:Se ratio higher than 1.. Regarding CdTe, cyclic voltammetry showed two peaks related to the reductive UPD of the $HTeO_2^+$ on Au(111), and they occur at potential too positive to be easily observed on Ag(111) due to its narrower electrochemical stability window. They are related to a complex chemistry well explained in the literature [16]; hence, it is necessary to use a scheme similar to the CdSe

growth. The charge deposited for the first Te layer on Ag(111) is equal to that found on the first UPD of Te on Au(111), for which a (12 × 12) structure was revealed by STM images as well as by low-energy electron diffraction (LEED) patterns. LEED measurements after emersion at a potential corresponding to the second UPD of Te also showed that the (12 × 12) structure originated from a (3 × 3) structure [17]. The structure formed in correspondence with the sole UPD of Te observed on Ag(111) is expected to have the same structure [18]. However, no morphological or structural analysis has been performed on such substrate in order to confirm the expectation. Eventually, E-ALD also gives the possibility of growing ternary and quaternary compounds, and here we describe the case of ternary chalcogenides $Cd_xZn_{1-x}S$ and $Cd_xZn_{1-x}Se$ grown on Ag(111) [19–21]. The stoichiometry of the ternary chalcogenides grown by E-ALD can be controlled by the ZnX/CdX (X = S, Se) ratio. Still, CdX deposition seems to be favored with respect to ZnX deposition, hence the ratio between Cd and Zn cycles in the E-ALD sequence does not correspond to the stoichiometric ratio of Cd and Zn in the ternary compounds. Zn-deficiency is a general trend in ternary compounds deposited by means of E-ALD. The authors reported that the most likely explanation for the experiments is a lower deposition rate for Zn. However, electrochemical and XPS characterization confirmed the layer-by-layer growth and the 1:1 ratio between metals and sulfide ions. Eventually, the thickness seems to decrease while decreasing the Cd content. Analogous behavior, although referred to films as thick as 1–5 μm, was found for the compounds grown by the dip technique [22].

2.1.3. An overview on thermodynamics and lattice mismatches

The potential shifts exploited by the SLR involved in the E-ALD steps are related to the driving force of the process. As discussed in the first part of this text, the definition of the driving force is an open question for the E-ALD, and we can divide it in three terms:

1. The interaction with the surface.
2. The formation of a compound (ΔE_f related to the free energy of formation).
3. The cumulative elastic energy (ΔE_{mis}).

The first term probably dominates the first stages of the growth, while for films with a thickness of several E-ALD cycles the second and third terms become predominant. Experimental results on similar electrodeposition process reported by Golan showed that the growth of such thin films can be either stopped [23, 24] or develop overgrowing quantum dots due to their cumulative strain. Hence, for a qualitative analysis on thin films of practical interest, we consider the potential shift related to the following energy term:

$$\Delta E = \Delta E_f + \Delta E_{mis} \tag{1}$$

where ΔE_f is the chemical energy related to the formation of the CdX compound, ΔE_{mis} is the cumulative elastic energy of the overgrowth due to the mismatch with the substrate. Considering m:n supercells structure, the mismatch is the following:

$$M = \frac{n\,a_o - m a_s}{n\,a_o} \tag{2}$$

where *n* is the index of the supercell for the overgrowth, while *m* is for the substrate. As a rule of thumb, we consider larger supercells energetically less stable, even though their mismatch can be smaller. Eventually, an assessment of the cumulative elastic energy is impossible due to the lack of force constants for the hexagonal phases of the system CdX (*x* = S, Se and Te). Still, **Table 1** reports an overview of the ΔE_f and the mismatch for Ag and Au along selected orientations. Some of these structures have been experimentally verified in literature. Shannon and Demir [14] and Golan et al. [25] reported for CdS over Au(111) a 3:2 supercell with higher mismatch than the 10:7. Despite the lower mismatch of last supercell, we think this is probably related to the lower cumulative elastic energy involved in the latter due to its lower supercell index.

In principle, E-ALD of CdTe should result in a very stable compound. However, the elastic strain induced by the lattice mismatch is higher than the other two chalcogenides, unless we take into considerations very big supercell. On the other hand, CdSe seems to have very favorable chemical and elastic terms for the growth over both the substrates. Still, the experimental condition for a 1:1 growth is not easy to achieve due to the electrochemical behavior of Se. Eventually, Cd and S have a very straightforward electrochemical behavior over Ag(111). The growth of CdS on Ag(111) and Au(111) substrates is quite strained (≈4–5%) unless the substrate and compound are rotated by 30° with respect to the other. Moreover, two structures for the CdS compounds with a very similar stability are known, wurtizte-like (hexagonal—grenockite) and zincblende-like (cubic—hawleyite). Hence, the growth and structure for CdS are suitable for the characterization by SXRD. In conclusion, SXRD is a natural follow-up for the characterization of these films due to its coupled surface and bulk selectivities. In particular, CdS resulted to be an ideal system for performing operando studies of E-ALD growth.

2.2. Copper-based sulfides

Copper sulfides are considered very interesting for their particular transport and electronic proprieties. Several phases in the Cu-S compositional field have been reported to have a band gap suitable for photovoltaics. Moreover, covellite (CuS) is a natural superconductor and chalcocite (Cu_2S) is a superionic conductor. In the attempt to modulate the band gap of Cu_2S, a Zn-doped compound semiconductor (Cu_xZn_yS) has been deposited. Hence, recently, the research focused on Cu_2S and Cu_xZn_yS with some operando SXRD studies. In some cases, the epitaxial growth of thin films or 2D structure has been characterized. Revealing the peculiar structural proprieties of these materials. Moreover, these studies confirmed the advantage in using E-ALD as a production techniques for these systems in terms of growth control and quality of the resulting structure.

	$\Delta G_f°$ (KJ/mol)	M Ag(111)	M Au(111)	M Ag(111)R30°	M Au(111)R30°
CdS	−92.0	3:2 4% (10:7 −0.6%)	3:2 5% (10:7 −0.7%)	5:6 0.5%	5:6 0.3%
CdSe	−148.6	3:2 0.8%	3:2 0.6%	5:6 0.5% (6:7 0.2%)	5:6 −3% (6:7 −0.4%)
CdTe	−156.5	3:2 −5% (8:5 1%)	3:2 −5% (8:5 0.9%)	5:6 −9% (11:12 0.3%)	5:6 −9% (11:12 0.1%)

Table 1. Mismatches for Cd chalcogenides on different epitaxial relationship for Ag(111) and Au(111) substrates.

2.2.1. Copper sulfide (Cu_2S)

Copper sulfide thin films were grown on Ag(111) by means of E-ALD, hence alternating the UPD of S and Cu. A reliable assignment of the structure and stoichiometry for these semiconductor compounds is very difficult because of the variety of stable known structures in the Cu-S compositional field. Moreover, the electrochemical behavior of Cu on the Ag(111) substrate is quite complex. In fact, Cu cannot be deposited by means of UPD on Ag(111), [26], however the compound can be obtained by deposition of Cu on the S covered Ag(111) surface. Moreover, the electrochemistry of Cu(II) in ammonia buffer involves a number of interconnected reactions that must be taken into account [26]. It has been found that there are clearly predominant processes in this set of four possible reactions whose equilibrium changes according to the applied potential. It is reported that on silver Cu(II) is immediately reduced to Cu(I), and the formation of Cu(0) from Cu(I) reduction occurs at less negative potentials than that from Cu(II) [26]. Hence, experimental data reported by Innocenti et al. support the hypothesis of an SLR deposition as a result of the competitive process between these four reactions [26]. Like for CdTe and CdSe, such complex chemistry of the SLR hinders the strict assignment of the E-ALD step as an UPD process. However, even depositing Cu and S using surface-limited depositions, more complex in nature, the electrochemical and compositional analyses confirmed that we succeeded in growing multilayers of Cu_2S. Regarding the valence state of the elements in the compound, Cu(I) is present in both Cu_2S and CuS, which are the endmembers of the Cu-S compositional field. Hence, one cannot easily distinguish the two phases by means of an analysis of the binding energy as measured with XPS. In fact, Cu(I) and Cu(II) have almost coincident energy in the XPS, while both sulfide and disulfide peaks have been found in the spectra [27]. Hence, on this basis, the assessment of the stoichiometry associated with the Cu_2S cannot be safely discussed. Moreover, the short-range structural analysis carried by means of extended X-ray absorption fine structure (EXAFS) reported a first shell compatible with chalcocite structure (Cu_2S) for similar systems (Cu_xZn_yS) [28]. The electrochemical characterization also allows to establish that the same amount of compound is deposited in each deposition cycles, thus indicating the layer-by-layer growth mechanism that was the goal to achieve. Eventually, AFM analysis for 20 E-ALD is able to evidence the low roughness values of our deposits (4 Å), still higher than CdS [26].

2.2.2. Cu_xZn_yS

Although mixed Cu-Zn sulfides are supposed to be obtained as a solid solution [5], just few studies claimed to have synthesized CuZnS and (Cu, Zn)S, respectively [29, 30], without a conclusive proof. It is known that the electrodeposition of alloys and compounds allows to deposit metastable phases, thus the E-ALD approach can be a good way to grow Cu_xZn_yS films. The E-ALD process for Cu_xZn_yS follows the alternate deposition of Cu_xS and ZnS layers. The films obtained applying the general sequence Ag/S/[(Cu/S)/(Zn/S)m)]n with several different (m,n) were fully investigated by means of electrochemical characterizations. Chemical composition of the film obtained with (n,m) = (1,40) E-ALD cycles indicated a Cu/Zn ratio of about 6. Thus confirming the low contribution of Zn in ternary compound already

evidenced in the previous studies [6, 19, 31]. Eventually, Cu_xZn_yS was grown by E-ALD with a stoichiometry changing linearly with m at constant S layers (n x m); hence, the stoichiometry can be tuned by the ZnS/CuS deposition sequence. By means of extrapolation, the authors report that the 1:1 ratio can be achieved with $n = 13$ meaning a strong deficiency of Zn in the sulfides. This could be explained by a partial redissolution of zinc during the deposition of copper, which could also cause a rearrangement in the deposited materials. This is known to happen in similar methods such as the selective electrodesorption-based atomic layer deposition (SEBALD) method [32]. It is worth notice that at least two prevailing morphologies and two different crystal structures were highlighted by SEM-EDX and XAS investigations [28]. If grown alone, the Cu_2S and ZnS films reveal thin film morphology. For Cu_xZn_yS, it is reported that the occurrence of nanowires can be attributed to the lack of miscibility between the Cu and Zn sulfides [28, 33–35]. On the basis of the experimental results, E-ALD is proposed to progressively cover the Ag (111) surface with a nanometric polycrystalline film consisting of oriented microcrystals [2, 5–7, 27, 31]. However, in some case, it is possible to obtain polycrystalline phases when depositing ternary compounds or solid solutions of binary compounds that are not completely miscible [28].

2.2.3. CdS/Cu_xZn_yS

Recently, it has been reported that the first successful deposition of a CdS layer on the top of Cu_xZn_yS deposits was over a Ag(111) electrode by means of E-ALD [36]. This is a remarkable achievement despite the process resulted as highly complex. Thus, the final attribution of a SLR deposition for Cd has been achieved in an unconventional way due to the overlap of the oxidative stripping potential of Zn and Cd. This conundrum has been overcome taking into account two deposition processes that were different with respect to the potential related to a small bump in the CVs: (1) potentiostatic in underpotential conditions and (2) potentiostatic in slightly overpotential conditions. The charge deposited by means of the two procedures to the deposition of the partial atomic layer of Cd over a sulfide substrate [8, 37] confirming the process as an effective SLR Cd deposition. Moreover, thanks to the XPS investigations, the occurrence of a complex sample composition (including the eventual presence of ZnS oxidation and/or the alloying between CdS and ZnS) is revealed. Finally, XPS measurements suggest that the structure is layered as expected from the E-ALD process applied to the growth of a p-n junction.

3. Experimental setups for operando experiments

3.1. Solutions

Both metal ions and chalcogenides solutions for the process are prepared with analytical reagent grade without further purification. Buffer solutions are prepared with double-distilled water and analytical reagent-grade acid and bases. Commonly, a buffer of $HClO_4$ (65%) and NH_4OH (33%) is used to freshly prepare solutions of the metal and chalcogenides ions at very small concentration (typically 0.5 mM).

3.2. Electrodes

Several works report E-ALD of semiconducting materials over a polycrystalline substrates, although very interesting, this films cannot be analyzed by means of the SXRD technique. In this context, very common substrates are Au or Ag single crystal with almost every low index facets as electrodic surface. We focus on the last, which is less noble, but less expensive, even though it requires a specific treatment of the surface to enable its use as a substrate. Moreover, as shown by our group, it is possible to correctly orient its crystals to low index planes with an easy and inexpensive procedure. Silver single crystal spheres can be grown in a graphite crucible according to the Bridgman technique. The crystal is strongly etched exposing the low index facets with a good contrast at the macroscale and a visual detection of the crystal orientation can be made [38]. These procedure is quite reliable, and most common problems are related to the growth step with the Bridgman technique. This step leads to very pure materials, but the resulting silver single crystal could have a concentration of defects unsuitable for the SXRD setups. So, the growth of the crystal needs to be carried very carefully in order to ensure the necessary quality of the electrodes. After the cut, the electrodic surface is polished with emery paper and successively finer grades of alumina powder down to 0.05 μm. Before each measurement, the electrodes are cleaned with water in an ultrasonic bath for 15 min and chemically polished using a patented procedure based on CrO_3. The surface roughness can be improved in ultra-high vacuum by performing several sputtering-annealing cycles.

3.3. Automated system

An automated system for the exchange of solution in the electrochemical cell was first built at the University of Florence and European synchrotron radiation facility (ESRF) workshops, enabling the deposition of several layers, up to 120 E-ALD, in few hours. The automated system has been implemented at the ID03 and ID32 beamlines of the European synchrotron radiation facility (ESRF) in Grenoble, France. The apparatus consists of pyrex solution reservoirs, solenoid valves, a distribution valve, and a flow-cell. The whole is under fully automatic computer control [12].

3.4. The flow cell

Improvements with respect to thin-layer cells have been made designing a cell with suitable windows and flow channels enabling the fast exchange of the solutions [12]. The working electrode is placed at the bottom part of the cell that is directly fastened to the sample holder of the diffraction beamline front end. This position is particularly convenient for the alignment of the electrode surface and for exposure to the X-ray radiation. Although a careful choice of the material has to be done, the electrochemical cell can be built with Teflon, Kelef, or other chemically resistant plastics. Among others, PEEK is gaining favor in the field of operand SXRD measurement due to its resistance to hard X-ray radiation. However, the PEEK suffers for the presence of some crystalline domains, and without an adequate design of the cell walls, the powder and amorphous patterns from the cell windows can hinder with the X-ray signal from the sample itself. We report the design defined by the joint work of the University of Florence and ESRF workshops in **Figure 2**.

http://dx.doi.org/10.5772/67355

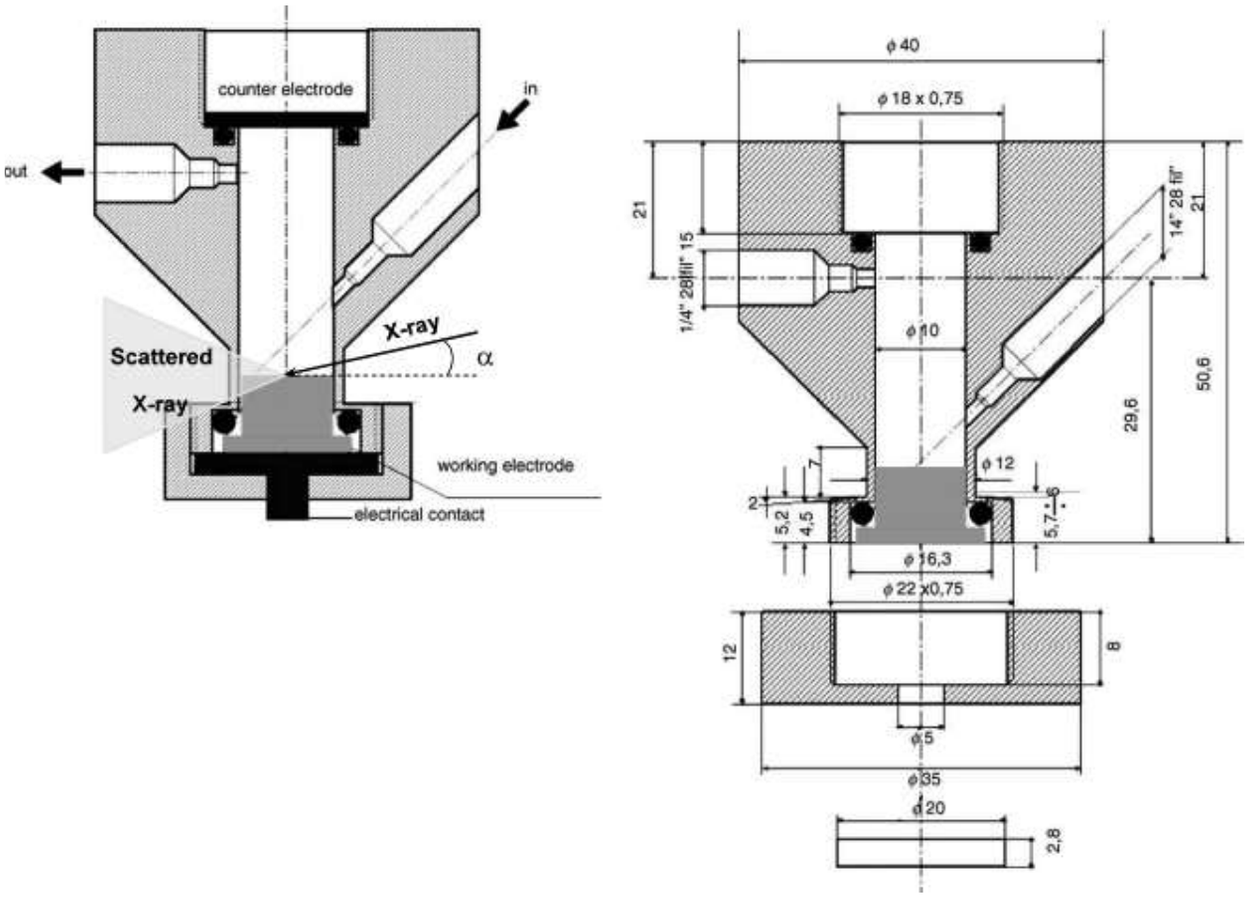

Figure 2. Technical specification for an electrochemical flow cell used in operando SXRD experiments.

The internal vessel is a cylinder with an internal diameter of 6.7 mm and a height of 40 mm. The electrochemical cell volume (1.5 mL) was delimited by the working electrode on one side and the counter electrode on the other side. The inlet and the outlet for the solutions were placed on the side walls of the cylinder. The counter electrode was a gold foil, and the reference electrode made of a small Ag/AgCl (KCl sat.) is placed in the outlet pipe. The attenuation of the X-rays along the typical path for an SXRD experiment can be estimated considering the absorbed radiation through a typical optical path as reported in **Figure 2**. Considering an incident angle with the wall and the electrolyte very close to 90°, **Figure 3** reported different thickness and material for the X-ray window in the cell, while the optical path in the electrolyte does not change in the different setups taken into consideration. The X-ray beam propagates through two walls 100 μm–1 mm thick and roughly 10 mm of water. In the following paragraphs we report two SXRD setups, one involving a Teflon cell (for CdS experiments, Section 4.1) and then a PEEK cell (for Cu_2S experiment, Section 4.2). For the first CdS experiment, it has been reported that a cell was made of Teflon, with a wall of 1 mm. At 20 keV, for this setup, **Figure 3** reports an overall transmission across the X-ray windows and electrolyte of roughly 40%, which is well matching the data reported in the literature (50%) [12]. PEEK ensures a lower attenuation of diffracted signal. Moreover, PEEK windows can be reduced to 100 μm thanks to its better mechanical proprieties. Hence, as depicted in **Figure 3**, this setup ensures a transmission very close to 70% at 24 keV. It is worth noticing that PEEK has a strong X-ray diffraction, reducing the thickness of the X-ray window by a factor of 10, makes completely undetectable the signal diffracted by PEEK.

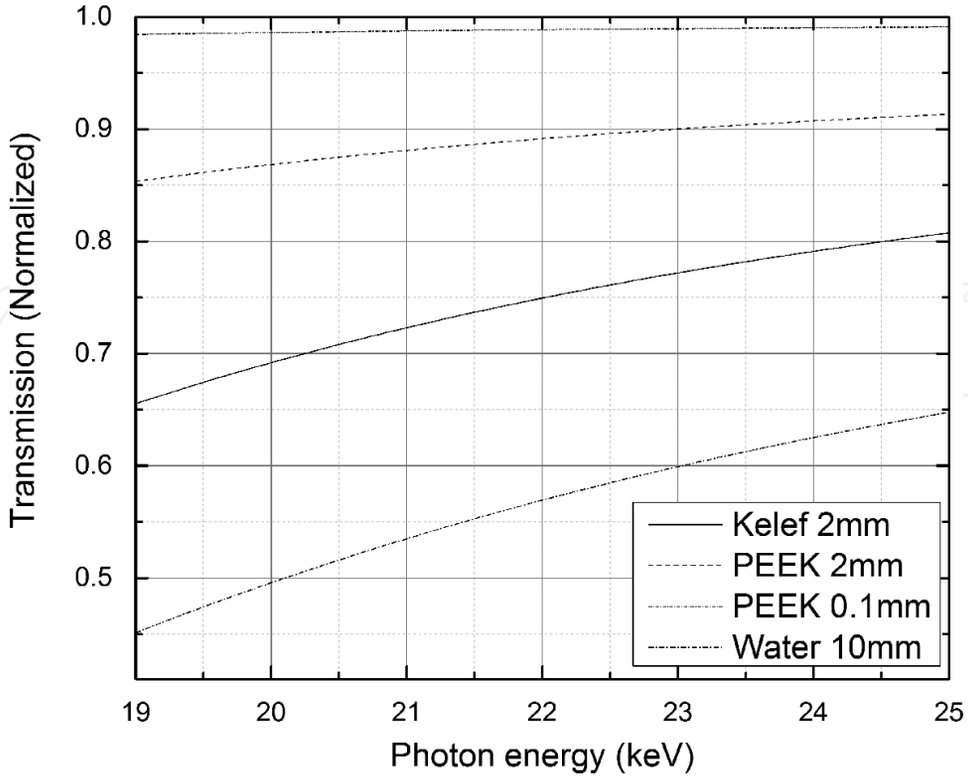

Figure 3. Transmission of X-ray at different energy through different surface.

We should report that the state-of-the-art E-ALD systems are also commercially available for the deposition of bigger electrode up to 4 cm^2, mainly used for polycrystalline substrates.

4. E-ALD and the sulfides structure

In this work, we report the intensity with respect to a coordinate system referred to as the pseudohexagonal surface unit cell of the Ag(111) substrate, in which the surface unit-cell parameters (a, b, c, α, β, γ) are defined so that the a and b vectors lay on the sample surface along the standard fcc [1 −1 0] and [−1 1 0] directions, while the c vector is perpendicular to the surface and parallel to the fcc [111] direction. The amplitude of the three vectors is given by the following relation together with the main surface cell angles.

$$\alpha = \beta = 90°, \gamma = 120°, |c| = \sqrt{3}\, a_0, |a| = |b| = \frac{a_0}{\sqrt{2}} \quad (3)$$

where a_0 is the lattice parameter of the cubic fcc cell of Ag. In the following, we adopted a reciprocal space metrics where *h*, *k*, and l are parallel to the a*, b*, and c* vectors of the reciprocal surface cell. In the following, we present two case studies on the CdS and Cu_2S comparing the results and the different applications of the SXRD due to different scientific questions that have to be answered for a better understanding of the E-ALD growth of these two materials.

4.1. CdS

E-ALD (or in this case ECALE) of CdS on Ag(111) has been involved in the testing of the experimental setup for in situ experiments by means of comparison of the structural results with theory and STM measurements. Moreover, the setups enabled structural determinations of the deposited film at different growth stages. In the first experiments at 20 kV performed by Giusti et al. [12], the reported attenuation is 50%, well matching with the attenuation curves reported in this work. The in situ diffraction measurements at controlled potential allowed the analysis of the CTRs for both the Ag(111) substrate and the Ag(111)/S surface. The fit of the CTRs showed that the last Ag layer on the bare metal has a contraction of 0.013 ± 0.008 nm toward the bulk. A vertical relaxation of the surface layer is observed in several (111) surfaces of noble metals and is due to the lack of bonding electrons at one side of low index surfaces [39]. Experimental works carried out on surfaces with a small roughness show an undetectable contraction of the surface layer [40, 41]. However, Ag(111) the contraction of the top layer is expected to strongly depend on the surface roughness [42]. A β-model has been involved in the fitting of the CTRs in order to take into account the surface roughness by means of fractionally occupied layers residing above the topmost complete one. In order to directly express the roughness in a length unit and not with a probability number, we can calculate the root-mean-square roughness σ, which can be calculated on the base of the Robinson model [43]. The oxidative absorption of S onto the Ag(111) surface induces strong modification on the shape of the CTRs. In fact, the best fit confirmed the top Ag layer with a site occupancy of 0.47 ± 0.07, in very good agreement with an S monolayer forming the (√7 × √7)R19.1 supercell as determined by STM images under electrochemical control at the same applied potential [44].

Hence, this setup for SXRD measurement has been successfully compared with literature data. In this context, this setup enabled the structural analysis in a straightforward manner. Wurtzite and zincblende have a very similar diffraction pattern, and they differ by the (200) reflection for zincblende and the (101) and (103) reflections for wurtzite. On this ground, X-ray diffraction data collected either in situ or ex situ, revealed that the films always present an ordered wurtzite structure with the *c*-axis perpendicular to the surface, confirming the epitaxial growth of CdS by means of ECALE on the Ag(111) substrate. In plane, different privileged orientations have been observed indicating that the first S layer structure might play a crucial role for the structural order of the grown films. Moreover, the X-ray reflectivity measurements collected in situ during the ECALE deposition of the CdS film, pointed out the correct 1:1 stoichiometric ratio between Cd and S and showed that the film thickness increases proportionally to the number of deposition cycles. Recent in situ SXRD experiment about the growth of CdS on Ag(100) and Ag(110) has been reported by Carlà et al. [13] confirming the epitaxial growth also on these substrates. On Ag(100), CdS has been found to be wurtzite-like, with two domain rotated by 30° with respect to the other and rotated by 15° and 45° with respect to the quadratic surface cell of the Ag(100) facet. While on Ag(110), the growth of CdS involves both zincblende (one domain) and wurtzite structures (two domains). The wurtzite domains on the Ag(110) are rotated by 30° with respect to the other and aligned with the substrate's main axis. Besides, for Ag(111), a different relative orientation of the two wurtzite domains is reported. These works clearly showed the influences of the substrate orientation on the CdS structure. Moreover, electrochemical measurements on Ag(100)

and Ag(110) indicate that the charge associated with each CdS and S layer has an average value comparable to that found for films grown on Ag(111). In this context, the XRR data were fitted including a roughness factor in the fitting parameter calculated according to the Névot and Croce formalism [45–47]. The resulting film thickness has been found to be 52.5 ± 0.5 Å on Ag(110) and 46.5 ± 0.5 Å for Ag(100), while the theoretical value is 100.7 Å. To better explain the experiments, the authors suggest that the UPD process can be considered a dynamic process occurring in steps where rearrangements and reordering of the atoms can take place. For a detailed description of this interpretation, the reader should refer to Ref. [13]. Still, these experiments constitute another confirmation that the film thickness and stoichiometry can be controlled by the number of ECALE cycles, even on different facets.

4.2. Cu_2S

As reported in Section 2, chemical composition, local structure, and stacking sequence suggest that the E-ALD process would require numerous reorganization steps. SXRD experiments showed no Bragg peaks or Debye rings during the first deposition cycles for Cu_2S. A clear difference with respect to the CdS, probably related to the lower scattering factor of Cu with respect to Cd and the more structural complexity that can be found in the Cu-S compositional field. The Cu-S mineralogical system is structurally and compositionally highly complex including five different structures between the two endmembers, CuS (Covellite) and Cu_2S (Chalcocite). Thus, for this material, it is more difficult, though crucial, to understand its crystalline structure. In a recent paper, our group took into consideration the more stable and geometrically suitable structures in this system. Thus, the published structural results are not conclusive, and other experiments and analysis are in progress. However, recent operando SXRD data acquired for a sample of 80 E-ALD cycles show a hexagonal structure, although a low symmetry structure has been reported. Hexagonal planes are present in the structures of both the possible candidates for the interpretation of the SXRD data. Moreover, in both cases, the *c*-axis of the substrate and of the film coordinate system is parallel. Chalcocite structure has layers (not planes) made of distorted hexagons, a perturbation of these distorted hexagons to make them proper hexagons gives a plane with a hexagonal pattern of sulfur atom. In contrast, Covellite has a hexagonal plane with a much shorter bond length than the Ag hexagonal plane leading (see **Table 2**); the expected strain is compressive of −1.1% along the main Ag(111)R30 –3 × 4 reconstruction directions, while for chalcocite, the strain is expansive of 1.0% along the Ag(111)R30 –4 × 5 reconstruction direction. It is also worth noticing that chalcocite is far more stable than Covellite.

We proposed an attempt to map the indices of a chalcocite structure (Cu_2S) grown on Ag(111), based on two different orientation (Ag(111) and Ag(111)R30) with respect to the substrate. Although the chalcocite structure constitutes a suitable model for the Cu_2S, deposited by means of E-ALD, the transformation between the two crystallographic coordinates systems lead to unsatisfactory results.

Ag(111)	Covellite (CuS)	Chalcocite (Cu_2S)
2.889 Å	3.794 Å	~3.963 Å (mean of S–S distance of the hexagonal plane)

Table 2. Characteristic length of possible CuS /Ag(111) and Cu_2S /Ag(111) surfaces.

http://dx.doi.org/10.5772/67355

The periodicity along the zonal axis (Ag[111]) is reported in **Figure 4** by means of experimental l-scan in situ and ex situ. The periodicity along Ag[111] corresponding to an interplanar distance of 6.75 Å, very close to the half of the periodicity along c is as observed for the chalcocite [48]. The simulated l-scan correspond to a model constituted by the hexagonal compact packing of sulfur atoms with the same periodicity. The comparison between experimental and simulated l-scans confirmed the correspondence between the chalcocite structure and the structure of the sample along the Ag[111] axis when measured in situ, revealing the presence of another structure in the sample when measured ex situ. In order to highlight the origin of this structural evolution, the Bragg peak at (0.73 0.73 1.04) has been acquired in real time. The structure seems to change in a partially reversible manner while reaching the open circuit potential from the last applied potential. Comparing the data with the covellite structure, the periodicity along the *c* axis of the covellite is found to be not matching (16.34 Å). Moreover, the periodicity presented in **Figure 4** corresponds to a distance of 3.37 Å between two adjacent sulfur layer. Since the S–S distance is "modulated" by the presence of copper atoms (Cu:S ratio) in the Cu-S compositional field, according to Bolge, the measured distance should correspond to a stoichiometric ratio of 2:1(Cu:S) [49]. Although the periodicity of the sample along Ag[111] is well reproduced by chalcocite, on the plane covellite and chalcocite have similar expected strains (1%) for Ag(111)R30°. These data suggest chalcocite (Cu_2S) as a better model than covellite (CuS) for Cu_2S. However, the definition of a new structure forming the chalcocite one is needed to be able to conclusively describe the structure of this material. Even though the crystallographic structure of the sample is not clarified, the diffracted intensity on selected Bragg peaks during the in situ experiment increases monotonically as shown in **Figure 5**, thus confirming the growth of the films during the whole process.

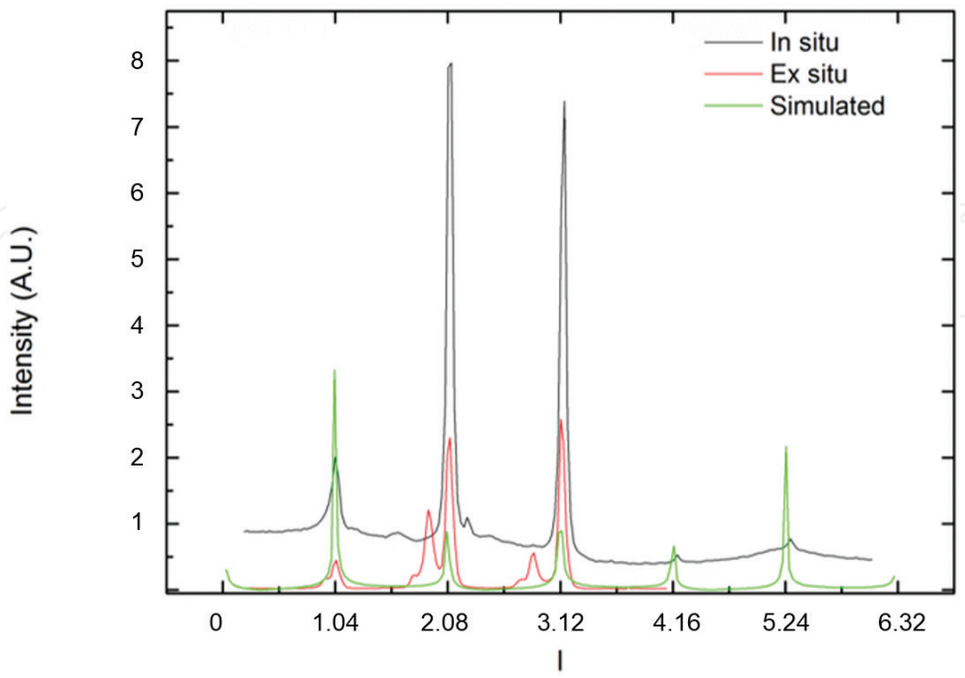

Figure 4. Operando (in situ), ex situ, and simulated l-scans (0.73, 0.73, l).

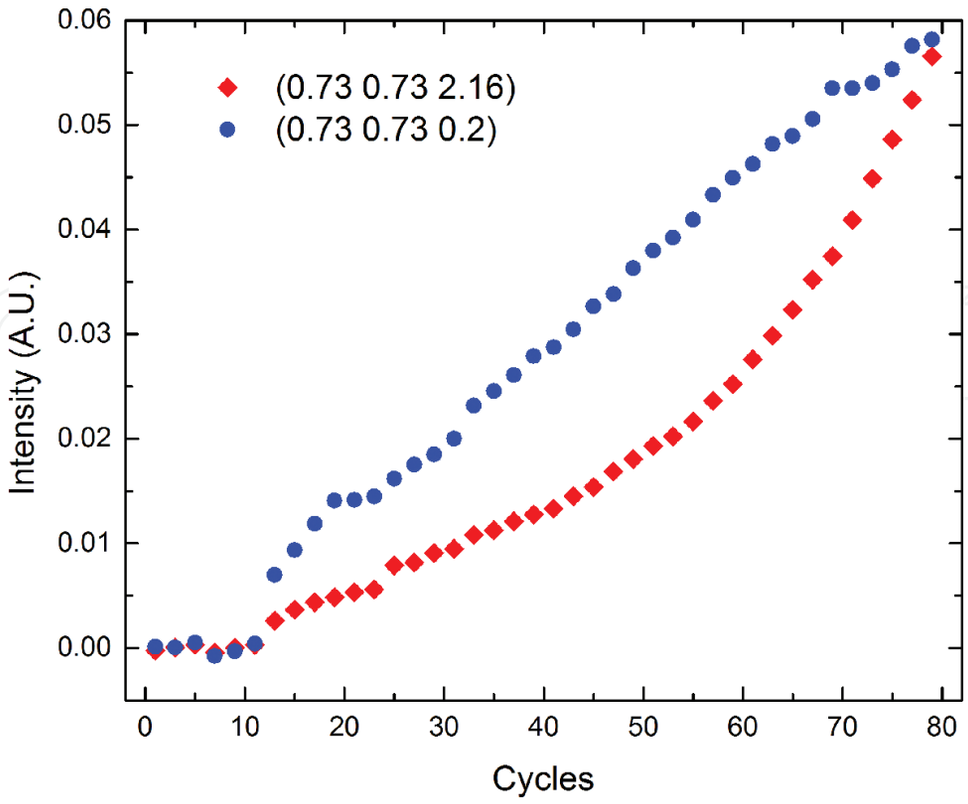

Figure 5. Diffracted intensity during the growth of Cu_2S ultra-thin film.

5. Conclusion

The first systems studied with operando SXRD has been chosen for their simple chemistry and because they had already been widely characterized with standard electrochemical and spectroscopical characterizations. By performing the operando SXRD, we have been able to address several open questions dealing with the effective growth process, the structures, the thicknesses, and the stoichiometry. SXRD has also successfully employed in the case of ultra-thin films grown by E-ALD, allowing to detect the surface reconstructions present in the first stages of the growth for CdS. The determination of thickness by means of the crystal truncation rods and reflectivity analysis revealed a very clear picture regarding the growth process of CdS, which is substantially different with respect to a mere layer-by-layer growth. In the case of Cu_2S, operando SXRD has revealed that the film crystallographic structure evolves as soon as the control potentials are removed from the cell with a time dynamics of few seconds. This structural transition is partially reversible if the applied potential is restored. Eventually, scanning along some selected reciprocal directions and taking advantage of the real-time acquisition of the diffraction intensity during the electrochemical evolution of the system allowed to understand both the structure and the stability of the Cu_2S. This gives the possibility of gathering information concerning the stoichiometry and its assessment by other techniques. In fact, for the Cu-S system, there is a very well-defined relationship between the structure and the Cu:S ratio; its stability revealed why the stoichiometry is coming from

ex situ XPS or why stripping voltammetry is not comparable with the stoichiometry coming from operando structural investigations. The unexpected stoichiometry of the film for Cu_2S raises several questions about the stability of this system. In conclusion, the operando SXRD results concern both CdS and Cu_2S while confirming the possibility of growing highly ordered ultra-thin films with high reproducibility, and they set a new interesting challenge for the fundamental surface science in explaining the complex mechanism, which is behind the growth of crystal by means of E-ALD.

Author details

Andrea Giaccherini[1]*, Roberto Felici[2] and Massimo Innocenti[1]

*Address all correspondence to: andrea.giaccherini@unifi.it

1 Department of Chemistry, University of Florence, Sesto Fiorentino, Italy

2 Istituto SPIN - CNR, Rome, Italy

References

[1] B.W. Gregory, J.L. Stickney. Electrochemical atomic layer epitaxy (ECALE). J. Electroanal. Chem. 1991;**300**:543–561.

[2] M. Innocenti, G. Pezzatini, F. Forni, M.L. Foresti. CdS and ZnS deposition on Ag (111) by electrochemical atomic layer epitaxy. J. Electrochem. Soc. 2001;**148**:C357–C362.

[3] M. Innocenti, F. Forni, G. Pezzatini, R. Raiteri, F. Loglio, M.L. Foresti. Electrochemical behavior of As on silver single crystals and experimental conditions for InAs growth by ECALE. J. Electroanal. Chem. 2001;**514**:75–82.

[4] F. Loglio, M. Innocenti, A. Jarek, S. Caporali, I. Pasquini, M.L. Foresti. Nickel sulfur thin films deposited by ECALE: Electrochemical, XPS and AFM characterization. J. Electroanal. Chem. 2010;**638**(10):15–20.

[5] M. Innocenti, L. Becucci, I. Bencistà, E. Carretti, S. Cinotti, L. Dei, F. Di Benedetto, A. Lavacchi, F. Marinelli, E. Salvietti, F. Vizza, M.L. Foresti. Electrochemical growth of Cu-Zn sulfides. J. Electroanal. Chem. 2013;**710**:17–21.

[6] F. Loglio, M. Innocenti, G. Pezzatini, M.L. Foresti. Ternary cadmium and zinc sulfides and selenides: Electrodeposition by ECALE and electrochemical characterization. J. Electroanal. Chem. 2004;**562**(1):17–125.

[7] M. Innocenti, L. Becucci, I. Bencistà, E. Carretti, S. Cinotti, L. Dei, F. Di Benedetto, A. Lavacchi, F. Marinelli, E. Salvietti, F. Vizza, M.L. Foresti. Ternary cadmium and zinc sulfides and selenides: Electrodeposition by ECALE and electrochemical characterization. J. Electroanal. Chem. 2013;**70**:17–21.

[8] M. Innocenti, S. Cinotti, I. Bencistà, E. Carretti, L. Becucci, F. Di Benedetto, A. Lavacchi, M.L. Foresti. Electrochemical growth of Cu-Zn sulfides of various stoichiometries. J. Electrochem. Soc. 2014;**161**(1):D14–D17.

[9] F. Di Benedetto, S. Cinotti, A. Guerri, A. De Luca, A. Lavacchi, G. Montegrossi, F. Carlà, R. Felici, M. Innocenti. Physical characterization of thin films of $Cu_xZn_yS_z$ for photovoltaic applications. ECS Trans.. 2013;**58**(11):59–65.

[10] M. Innocenti, F. Di Benedetto, A. Lavacchi, N. Cioffi, R. Felici and L.A. Pardi. Fabricating energy devices with low environmental impacts. SPIE Newsroom. 11 January 2016.

[11] K Rajeshwar. Electrosynthesized thin films of group II–VI compound semiconductors, alloys and superstructures. Adv. Mater. 1992;**4**:23–29.

[12] M.L. Foresti, A. Pozzi, M. Innocenti, G. Pezzatini, F. Loglio, E. Salvietti, A. Giusti, F. D'Anca, R. Felici, F. Borgatti. In situ X-ray analysis under controlled potential conditions: An innovative setup and its application to the investigation of ultrathin films electrodeposited on Ag(111). Electrochim. Acta 2006;**51**:5532−5539.

[13] F. Carlà, F. Loglio, A. Resta, R. Felici, E. Lastraioli, M. Innocenti, M.L. Foresti. Electrochemical atomic layer deposition of CdS on Ag single crystals: Effects of substrate orientation on film structure. J. Phys. Chem. C 2014;**118**:6132−6139.

[14] U. Demir, C. Shannon. Langmuir. 1994;**10**:2794.

[15] F. Loglio, M. Innocenti, G. Pezzatini, F. Forni, M.L. Foresti. Experimental conditions for CdSe layer-by-layer growth. In: P.C. Andriacos, P.C. Searson, C. Reidsema-Simpson, P. Allongue, J.L. Stickney, G.M. Oleszek. Electrochemical Processing in ULSI Fabrication III. Pennington, New Jersey: The Electrochemical Society; 2000. pp. 28–40.

[16] F. Forni, M. Innocenti, G. Pezzatini, M. Foresti. Electrochemical aspects of CdTe growth on the face (111) of silver by ECALE. Electrochim. Acta 2000;**45**:3225–3231.

[17] D.W. Suggs, J.L. Stickney. Studies of the surface structures formed by the alternated electrodeposition of Cd and Te on the low-index planes of Au: II. STM studies. Surf. Sci. 1993;**290**:375.

[18] B.E. Hayden, I. Nandhakumar. J. In-Situ STM Study of Te UPD Layers on Low Index Planes of Gold. Phys. Chem. B 1997;**101**:7751.

[19] F. Loglio, A. Telford, E. Salvietti, M. Innocenti, G. Pezzatini, S. Cammelli, F. D'Acapito, R. Felici, A. Pozzi, M. Foresti . Ternary $Cd_xZn_{1-x}Se$ nanocrystals deposited on Ag(111) by ECALE: AFM and EXAFS characterization. Electrochim. Acta 2008;**53**:6978–6987.

[20] F. Loglio, M. Innocenti, G. Pezzatini, M. Foresti. Electrochemical and morphological characterization of $Cd_xZn_{1-x}S$ electrodeposited on Ag(111) by ECALE. In: K. Kondo, D.P. Barkey, J.C. Bradley, F. Argoul, P.C. Andriacacos, J.L. Stickney, editors. Morphological Evolution of Electrodeposits-and-Electrochemical Processing in ULSI Fabrication and Electrodeposition of and on Semiconductors IV. New York, Washington: Kluwer Academic/Plenum Publishers; 2001. pp. 365–380.

[21] F. Loglio, M. Innocenti, G. Pezzatini, M. Foresti. Ternary cadmium and zinc sulphides and selenides: Electrodeposition by ECALE and electrochemical characterization. J. Electroanal. Chem. 2004;**562**:117–125.

[22] S.C. Ray, M.K. Karanjai, D. DasGupta. Deposition and characterization of ZnxCd1− xS thin films prepared by the dip technique. Thin Solid Films. 1998;**322**:117.

[23] Y. Golan, B. Alperson, I. Rubinstein, G. Hodes, J. L. Hutchison. Extended Abstracts-Electrochemical Society Meeting; May 1994; San Francisco. p. 94-1, 874, 1350.

[24] Y. Golan, L. Margulis, I. Rubinstein, G. Hodes, J.L. Hutchison. Proceedings of the 13th International Congress on Electron Microscopy. In: B. Jouffrey, C. Colliex, editors. July 1994; Paris. p. 2A, 345.

[25] Y. Golan, G. Hodes, I. Rubinstein. Electrodeposited Quantum Dots. 3. Interfacial Factors Controlling the Morphology, Size and Epitaxy. J. Phys. Chem. 1996;**100**:2220–2228.

[26] M. Innocenti, I. Bencistà, S. Bellandi, C. Bianchini, F. Di Benedetto, A. Lavacchi, F. Vizza and M.L. Foresti. Electrochim. Acta. 2011;**58**:599– 605

[27] I. Bencistà, F. Di Benedetto, M. Innocenti, A. De Luca, G. Fornaciai, A. Lavacchi, G. Montegrossi, W. Oberhauser, L.A. Pardi, M. Romanelli, F. Vizza and M.L. Foresti. Phase composition of Cu_2S thin films: Spectroscopic evidence of covellite formation. Eur. J. Miner. 2012;**24**:879–884.

[28] F. Di Benedetto, S. Cinotti, F. D'Acapito, F. Vizza, M.L. Foresti, A. Guerri, A. Lavacchi, G. Montegrossi, M. Romanelli, N. Cioffi, M. Innocenti . Electrodeposited semiconductors at room temperature: An X-ray Absorption Spectroscopy study of Cu-, Zn-, S-bearing thin films. Electrochim. Acta 2015;**179**:495–503.

[29] C.C. Uhuegbu, E.B. Babatunde, C.O. Oluwafemi. The Study of Copper Zinc Sulphide (CuZnS2) Thin Films. Turk. J. Phys. 2008;**32**:39-47.

[30] K.A. Aduloju, A.I. Mukolu. Optical absorption and transmission in CuZnS alloys. Glob. J. Pure Appl. Sci. 2009;**15**(3):421–425.

[31] M. Innocenti, S. Cattarin, F. Loglio, T. Cecconi, G. Seravalli, M.L. Foresti. Electrochim. Acta 2004;**49**:1327–1337.

[32] M. Innocenti, S. Bellandi, E. Lastraioli, F. Loglio, M.L. Foresti. Selective electrodesorption based atomic layer deposition (SEBALD): A novel electrochemical route to deposit metal clusters on Ag(111). Langmuir 2011;**27**(18):11704–11709.

[33] J.R. Craig, G. Kullerud. The Cu-Zn-S System. Miner. Depos. 1973;**8**:81–91.

[34] M. Miyauchi, T. Hanayama, D. Atarashi, E. Sakai. Photoenergy conversion in p-type Cu_2ZnSnS_4 nanorods and n-type metal oxide composites. J. Phys. Chem. C 2012;**116**:23945–23950.

[35] I.D. Olekseyuk, I.V. Dudchak, L.V. Piskach. Phase equilibria in the Cu_2S–ZnS–SnS_2 system. J. Alloys Compd. 2004;**368**:135–143.

[36] E. Berretti, S. Cinotti, S. Caporali, N. Cioffi, A. Giaccherini, F. Di Benedetto, M.L. Foresti, G. Montegrossi, A. Lavacchi, F. Vizza, R.A. Picca and M. Innocenti. Electrodeposition and characterization of p and n sulphide semiconductors composite thin film. J. Electrochem. Soc. 2016;**163**(12):D3034–D3039 .

[37] S. Caporali, A. Tolstogouzov, O.M.N.D. Teodoro, M. Innocenti, F. Di Benedetto, S. Cinotti, R.A. Picca, M.C. Sportelli, and N. Cioffi. Sn-deficiency in the electrodeposited ternary CuxSnySz thin films by ECALE. Sol. Energ. Mater. Sol. Cells. 2015;**138**:9.

[38] M.L. Foresti F. Capolupo, M. Innocenti, F. Loglio. Visual detection of crystallographic orientations of face-centered cubic single crystals. Cryst. Growth Des. 2002;**2**(1):73–77.

[39] R.J. Needs, M.J. Godfrey, M. Mansfield. Theory of surface stress and surface reconstruction. Surf. Sci. 1991; **242**: 215.

[40] M.F. Toney, J.N. Howard, J. Richer, G.L. Borges, J.G. Gordon, O.R. Melroy, D.G. Wiesler, D. Yee, L.B. Sorensen. Voltage-dependent ordering of water molecules at an electrode–electrolyte interface. Nature 1994;**368**:444.

[41] E.A. Soares, V.B. Nascimento, V.E. de Carvalho, C.M.C. de Castilho, A.V. de Carvalho, R.Toomes, D.P. Woodruff. Structure determination of Ag(111) by low-energy electron diffraction. Surf. Sci. 1999;**419**:89.

[42] N.H. de Leeuw, C.J. Nelson. A Computer Modeling Study of Perfect and Defective Silver (111) Surfaces. J. Phys. Chem. B 2003;**107**:3528.

[43] I.K. Robinson. Crystal truncation rods and surface roughness. Phys. Rev. 1986;**B33**:3830.

[44] M.L. Foresti, G. Pezzatini, M. Cavallini, G. Aloisi, M. Innocenti, R. Guidelli. Electrochemical Atomic Layer Epitaxy Deposition of CdS on Ag(111): An Electrochemical and STM Investigation. J. Phys.Chem. B 1998;**102**:7413.

[45] Software Reflectivity Tool Parratt 32; HMI: Berlin, 1999.

[46] L.G. Parratt . Surface studies of solids by total reflection of X-rays. Phys. Rev. 1954;**95**:359–369.

[47] L. Névot, P. Croce . Caractérisation des Surfaces par Réflexion Rasante de Rayons X. Application à l'Etude du Polissage de Quelques Verres Silicates. Rev. Phys. Appl. 1980;**15**:761–780.

[48] H.T. Evans. Crystal structure of low chalcocite. Nature Phys. Sci. 1971;**232**:19.

[49] R.J. Goble. The relationship between crystal structure, bonding and cell dimensions in the copper sulphides. Can. Miner. 1985;**23**:61–76.